fMRI visualisation of transient activations in the rat olfactory bulb using short odour stimulations

Martin, C. (a), Grenier, D. (b), Thévenet, M. (a), Vigouroux, M. (a), Bertrand, B.(a), Janier, M. (c), Ravel, N. (a) and Litaudon, P. (a), ,

(a) Neurosciences Sensorielles, Comportement et Cognition, CNRS UMR 5020 – Université Claude Bernard Lyon 1, IFR19, Institut Fédératif des Neurosciences de Lyon, Lyon, France

(b) Creatis LRMN, CNRS UMR 5220, U630 INSERM - Université Claude Bernard Lyon 1, INSA Lyon, IFR19, Institut Fédératif des Neurosciences de Lyon, Villeurbanne, France

(c) Plate-forme ANIMAGE (Rhône-Alpes Genopole), Bron, France

Correspondence: P. Litaudon, Neurosciences et Systèmes Sensoriels, Université Lyon I – CNRS, 50 avenue Tony Garnier, 69366 Lyon cedex 07, France

Tel.: (33) 4 37 28 74 61

Fax: (33) 4 37 28 76 01

e-mail: litaudon@olfac.univ-lyon1.fr

Abstract

Odour-evoked activity in the olfactory bulb OB displays both spatial and temporal organization. The difficulty when assessing spatio-temporal dynamics of olfactory representation is to find a method that reconciles the appropriate resolution for both dimensions. Imaging methods based on optical recordings can reach high temporal and spatial resolution but are limited to observation of the accessible dorsal surface. Functional magnetic resonance imaging (fMRI) may be useful to overcome this limitation as it allows recording from the whole brain. In this study, we combined ultra fast imaging sequence and short stimulus duration to improve temporal resolution of odour evoked BOLD responses. Short odour stimulations evoked high amplitude BOLD responses and patterns of activation were similar to those obtained in previous studies using longer stimulations. Moreover, short odour exposures prevented habituation processes. Analysis of the BOLD signal time-course in the different areas of activation revealed that odorant response maps are not static entities but rather are temporally dynamic as reported by recent studies using optical imaging. These data demonstrated that fMRI is a non-invasive method which could represent a powerful tool to study not only the spatial dimension of odour representation but also the temporal dimension of information processing.

Introduction

From the early 2DG experiments to the most recent optical imaging studies, a consistent finding has been that odorant compounds generate activity that is widely distributed across the glomerular layer of the olfactory bulb (OB). Hence, in this structure, the identity of odorants is associated with a unique spatial map of activity. In addition to spatial patterns, odour-evoked activity in the OB displays temporal dynamics when examined through local field potential. A prominent characteristic of the electrophysiological activity in the OB is the recording of slow waves of high amplitude related to respiratory modulation. These slow waves have been shown to influence the temporal pattern of mitral/tufted cell unitary activities (Buonviso et al., 2006). Coexisting with this slow modulation, rhythmic activities in higher frequency bands are present in the OB and have been proposed to play a role in odour coding (Buonviso et al., 2003, Martin et al., 2004).

The difficulty when assessing the spatio-temporal dynamics of olfactory representation is to find a method that reconciles the appropriate resolution for both dimensions. Relatively few imaging studies have used adequate methods to observe neuronal events in real time. Recent imaging studies using voltage-sensitive dye in the mammalian OB revealed odour-specific sequences of glomerular activation that were dynamic over time, pointing out that both odour identity and concentration are represented by spatio-temporal patterns, rather than spatial patterns alone (Spors and Grinvald, 2002; Spors et al., 2006). However, these methods based on optical recordings are limited to observation on the accessible dorsal surface.

Functional magnetic resonance imaging (fMRI) may be useful to overcome this limitation as it allows recording from the whole brain. Indeed, recent studies using fMRI based on blood oxygenation level-dependent (BOLD) image contrasts clearly demonstrated odour-elicited activity patterns in rat and mouse olfactory bulb (Yang et al., 1998; Xu et al., 2000, 2003). However, these studies did not focus on the temporal aspect of the responses. They used a

conventional gradient-echo acquisition sequence (FLASH) and relatively long stimulus duration (several tens of seconds) which limited the temporal resolution. Moreover, such long stimulations are known to induce habituation processes at different levels of the olfactory system (Wilson, 2000). The present report describes an initial series of experiments designed to improve temporal dynamic resolution of BOLD responses. In this study, we combined ultra fast imaging sequence (Echo Planar Imaging, EPI) and short stimulus duration similar to what is used for electrophysiological studies (Buonviso et al. 2003; Litaudon et al. 2003). Using this protocol, we successfully elicited short and localized BOLD responses revealing dynamic changes within seconds. These results are promising for future use of fMRI technique in rodents to study odour representation in the whole OB.

Material and methods

Animal preparation

All procedures were conducted in strict accordance with the European Communities Council guidelines. Experiments were performed on 11 male Wistar SPF rats (IFFA-CREDO, L'Arbresle, France) weighing 300-400 g. Recordings were carried out in naturally breathing, urethane (1.5 g/kg) anesthetized rats. Anaesthesia was maintained by supplemental doses when necessary. Before being inserted into the magnet, the rat was placed prone with its head maintained in a holder to minimize movements. A small non-magnetic pressure sensor was inserted under the animal body to record chestwall movements associated with respiration. Respiratory rhythm was monitored to ensure that respiratory frequency remained constant along the experiment and was used to trigger odour stimulation.

Odour stimulation

The odour (isoamyl-acetate, SIGMA) was delivered using a custom-built flow dilution olfactometer, at a concentration of ~ 5.10^{-2} of saturated vapour and at a rate of 1 litre/min. Stimulations lasted 5 sec and were separated from each other by at least 2 min. Stimulus onset was triggered on the respiratory cycle (near the maximum of the exhalation).

fMRI experiments

Imaging experiments were performed on a horizontal-bore 7T spectrometer (Bruker Biospec). A circular radio frequency surface coil probe (15 mm diameter) was centred between the two eyes to maximize the signal from the OB. Before the fMRI acquisition, 10 high resolution anatomical images slices of the OB were acquired using a RARE (rapid acquisition with relaxation enhancement) sequence with the following parameters: repetition time (TR)= 5500 ms; echo time (TE)= 76 ms; Field of view (FOV) 1.75 x 1.75 cm; matrix= 128 x 128, slice thickness=500 µm, voxel size: 137 x 137 x 500 µm. The multi-slice fMRI experiments were carried out using the EPI sequence with the following parameters: TR and TE were experimentally trimmed to respectively 1000 and 19.5 ms, this choice appearing to be the best compromise between the wanted T2* weighting, T1 weighting, and image quality for the 7T spectrometer used. Ten 64 x 64 pixels slices of 500 µm thickness for a 1.75 x 1.75 cm FOV (voxel size: 273 x 273 x 500 µm) were acquired each TR. The temporal resolution for the entire OB acquisition was 1 sec. 10 dummy scans were performed before each fMRI data acquisition to reach steady state and limit T1 effects.

Experimental protocol and data analysis

Each fMRI run consisted of a series of 60 volumes (10 slices, 1 sec/volume). 16 volumes were acquired as baseline volumes (Fig. 1). Odour stimulation was delivered for 5 seconds (5 volumes) after the 16^{th} volume. Usually, 15-20 functional runs were averaged to obtain a

single functional run. All functional images were analyzed off-line using Activis software (Thévenet and Cheylus, 2003). To avoid any bias in functional maps, neither data filtering nor image smoothing was performed during data processing and analysis. This experiment was based on a block design paradigm and data analysis consisted of the statistical comparison of the stimulation period versus the baseline period. Contrary to previous studies, short odour stimulation was used that elicited short responses. Therefore, analysis design and particularly the stimulation period needed to be carefully defined. As no model of the BOLD response exists for the rat, the stimulation period was defined according to the human canonical haemodynamic response function (HRF) (Fig. 1). Then functional maps were generated using contrast non-paired t-tests between stimulation and baseline periods (Fig. 1). These functional maps allowed us to define regions of interest (ROI) from which the BOLD signal time course was retrospectively computed.

In order to validate the use of a human canonical HRF to define our analysis paradigm, a pixel by pixel correlation analysis was performed between human HRF and the actual BOLD signal. Such analysis indicated at each voxel the statistical level of correlation between the actual fMRI signal and the model. Such correlation maps were compared with contrast t-maps previously obtained with the method described above.

Results

Figure 2A shows the pattern of activation evoked by isoamyl-acetate stimulation along the OB antero-posterior axis. As previously reported (Xu et al., 2000; Yang et al., 1998), we found BOLD activations mainly located in the outer layers of the OB. In all rats, a five second odour exposure elicited bilateral strong activation in two glomerular regions (Fig. 2A): a dorso-lateral region extending in the anterior two-thirds of the OB, and a medial region extending in the posterior two-thirds of the OB. In 55% of the rats (6 rats out of 11), the 5 sec

stimulation also elicited ventral activation in the posterior half of the OB. Features of the BOLD signal were investigated by computing the mean curve of the signal intensity of these three ROI. On average, the BOLD signal increased 2.8 ± 0.88 % and no statistical differences in BOLD signal amplitude were observed between the three ROI. Although averaging was necessary to compute statistical maps, scan-to-scan analysis (Fig. 2B) revealed that BOLD response was detectable on single scan. BOLD signal amplitude was then computed along repetitions (Fig. 2C). Results indicated no significant change (repeated ANOVA, n=14, p=0.34) suggesting that no habituation processes occurred.

In order to validate the reliability of our analysis paradigm, we compared contrast t-maps (Fig 2A) with correlation maps computed from a model of canonical HRF. As shown in figure 2D, areas of activation revealed by both methods closely resemble one another. In all rats, both analysis methods revealed patterns of activity in the dorso-lateral, medial and ventral part of the OB. We only observed slight differences in the size of each ROI. Such results indicated that both actual BOLD response and human HRF have similar time courses as shown in figure 2E. The responses only differed in their last part where the actual BOLD signal did not show a negative component (Fig. 2E).

The last part of our experiment was devoted to the analysis of the dynamic time course of OB activation. Data were analyzed from the six rats exhibiting activation in the three ROI (dorsal, medial, and ventral) previously defined (Fig. 2A). Overall analysis indicated that BOLD responses started with a delay of about 2 sec relative to stimulus onset, and peaked between 6 and 9 sec. When analyzed in each ROI, it appeared that although the BOLD response started simultaneously in the three areas, peak latency was delayed in the ventral area compared to dorsal and medial response (Fig. 3A). Due to the small sample size, we used a non-parametric

test to compare mean peak latency in the three ROI. Even though differences failed to reach significance, we observed a clear statistical tendency (p=0.07, Friedman two-way ANOVA) suggesting that the peak latency differed between the three activation areas. Post-hoc tests confirmed this statistical tendency and showed that peak latency of the ventral area tended to be delayed compare to other areas (Wilcoxon rank test, dorsal vs medial: p=0.36; dorsal vs ventral: p=0.10; medial vs ventral: p=0.06) (Fig. 3B).

Discussion

This work was a first attempt to improve the temporal resolution when measuring odour evoked BOLD response in the OB, by combining short stimulus duration with ultra fast fMRI acquisition sequence. Contrasting previous studies (Yang et al., 1998; Xu et al., 2000, 2003), we used short stimulus durations and elicited BOLD responses lasting only a few seconds. Such an experimental paradigm led to new constraints regarding signal analysis. Because we obtained transient responses, an appropriate temporal model was critical to perform accurate statistical analysis. Small animal brain imaging using fMRI has been developed recently and there was limited data regarding the time course of haemodynamic responses in sensory systems. As no data were available for rats, the timing of our analysis paradigm was based on a human canonical HRF which is a model commonly used in human fMRI studies. Contrast t-maps based on this analysis paradigm revealed areas of activation which were similar to those previously reported (see below). Moreover, the BOLD response time courses computed in these activation areas fitted with the human canonical HRF and peaked on a timescale predicted by the canonical function. In order to statistically validate this observation, we compared our data with results obtained from a correlation analysis based on the model of human HRF (Fig. 2D). This method, which is commonly used to analyze human fMRI data, consists of calculating the level of correlation between each voxel and the model function.

Both methods revealed activation patterns in the same three location, i.e. the dorso-lateral, medial and ventral part of the OB. Even if the extent of the regions of interest obtained with both methods could not be statistically compared as they resulted from different method of calculation, they appeared similar. Such results indicated that both methods were suitable to analyze transient BOLD responses in the rat OB and that human canonical HRF could be used as a model for analyzing sensory activation in rats, at least in the OB.

As previously reported, activation areas were found in outer layers of the OB that correspond to the olfactory nerve, glomerular and external plexiform layers (Yang et al., 1998; Xu et al., 2000, 2003; Schafer et al., 2005, 2006). In all tested rats, isoamyl-acetate elicited activation in dorso-lateral and ventro-medial parts of the OB, matching the pattern previously described (Xu et al., 2000; Schafer et al., 2005, 2006). In 55% of the animals, isoamyl-acetate stimulation also elicited activation in the ventral part of the OB as reported by Yang et al. (1998). Ventral activations were much more difficult to observe due to technical considerations. Indeed, the use of a surface coil presents both the advantage of a very good signal-to-noise ratio in its immediate vicinity and the disadvantages of a relatively small detectable area and a rapid signal drop off with depth. Using the 15 mm diameter surface coil, we observed a clear decrease in signal intensity in the ventral part of the OB (see figure 2A). This decrease in intensity led to a decrease in signal-to-noise ratio making the ventral activation patterns more difficult to observe. Thus, the lack of activation in the ventral area in most of the previous studies could be explained by their use of smaller surface coil. Amplitude of BOLD responses evoked by short odour stimulation was similar (Kida et al., 2002) or slightly smaller (Yang et al., 1998) than reported in previous studies using longer odour exposure. Variations could be explained by differences in odour stimulation (concentration, stimulus flow rate), sensitivity of the surface coil probe, and imaging

sequences. Moreover, the amplitude of responses evoked in the OB was in the same range as those reported in other sensory systems (Yang et al., 1996; Keilholz et al., 2004). Interestingly, scan-to-scan analysis revealed that BOLD signals elicited by short odour pulses were large enough to be visualized without scan averaging.

As fMRI experiments generally require signal averaging, we have to be careful with habituation processes that could appear with stimulus repetition. Indeed, Wilson (2000) showed that habituation processes could be induced in OB with relatively short odour stimulations (50 sec). Inspection of individual scans along repetitions confirmed that our experimental paradigm excluded the possibility of habituation processes occuring across repetitions.

Compared to previous fMRI experiments, the use of short stimulus duration combined with fast imaging sequence allowed, for the first time, to follow the dynamics of bulbar activation with a 1 second temporal resolution. Analysis of BOLD signal time-course in the different areas of activation revealed that the peak of the ventral BOLD response was delayed compared to dorsal and medial activation. Such a result confirmed that odorant response maps are not static entities but rather temporally dynamic as reported by recent studies using optical imaging (Spors and Grinvald, 2002; Spors et al., 2006). These authors observed a sequential activation of several glomeruli, which exhibited different activation time-courses. Obviously, the temporal resolution of BOLD fMRI was not in the same range as the one of voltage-sensitive dye imaging (millisecond time resolution). BOLD signal represented integration of bulbar activation across several seconds. Due to the slow temporal patterning of OB afferent activity related to respiration, the OB was repetitively activated during the stimulation period (Buonviso et al., 2003). That the BOLD signal exhibited slower time-courses across successive respiratory cycles as shown in figure 3B suggests that some glomeruli exhibited

slower activation time-courses. Such results provide new evidence that odours are represented by a combination of temporal and spatial patterns in the mammalian olfactory bulb.

The present paper demonstrated that fMRI is a non-invasive method which represents a powerful tool to study not only the spatial dimension of odour representation but also the temporal dimension of information processing. Although both temporal and spatial resolution remained limited compared to optical imaging methods, BOLD fMRI was not restricted to the dorsal surface of the OB and so allowed the observation of activation patterns in the whole structure including its ventral part. The acquisition parameters were imposed by the necessity to image the whole OB with the best spatial and temporal resolution compatible with the coil used and the MRI system. The in-plane resolution (272 x 273 µm) was slightly larger than the size of OB glomeruli (Royet et al., 1989) with activated areas corresponding to several contiguous glomeruli. Mapping at glomerular resolution (110 x 110 x 250 µm) has been performed using another acquisition sequence (Kida et al., 2002) but at the expense of the temporal resolution. In the present experiment, we showed that with a time resolution of 1 second, BOLD fMRI can assess dynamic changes associated with odour responses. This time resolution remains large compared to the duration of the breathing cycle (0.5-1 sec and 0.125-0.5 sec in anaesthetized and awake rat respectively) which appears to be a critical time window for odour discrimination (Uchida et al., 2003; Abraham et al., 2004; Rinberg et al., 2006). One way to decrease the repetition time is to focus the acquisition on activated areas. Unfortunately, decreasing the repetition time leads to a decrease in signal-to-noise ratio. Future signal-to-noise improvements using new RF (radio frequency) coils, such as phased array detection coils, will increase the statistical significance and further improve both spatial and temporal resolution. Lastly, it should be underlined that temporal resolution is largely limited by the sluggish nature of the haemodynamic response. Comparison between voltage-

sensitive dye imaging and intrinsic signal imaging (Spors and Grinvald, 2002) showed that the intrinsic signal response (related to haemodynamic changes) failed to follow the respiratory modulation of OB activity.

Since five-second stimulations evoked large BOLD responses, it might be possible to further reduce stimulus duration opening up the possibility for use of different experimental paradigms such as event related fMRI. Moreover, the use of short stimulus durations will enable more powerful comparisons with other measures of neuronal activity. Simultaneous intracortical recordings of neural signal and fMRI responses suggest that the haemodynamic response primarily reflects the neuronal input to the relevant area of the brain and its processing there rather than output activity transmitted by action potentials to other regions of the brain (for a review see Logothetis and Wandell, 2004). Results obtained in the rodent OB seem to agree with such a hypothesis as BOLD responses were mainly located in the input layer (glomerular layer).

Thus, the rat OB appears to be a good model with which to compare fMRI data and other measures of neuronal activity, particularly an electrophysiological approach. Indeed, this structure is easily accessible for MRI compatible electrode implantation. Nevertheless, simultaneous fMRI and electrical recording remains a great challenge particularly when using high-field magnets. An alternative and easier method is to perform electrical recordings in parallel, taking into account fMRI activation areas to define electrode location. In the context of the present study, it would be of particular interest to see if the electrophysiological activity recorded in the different activated areas displays different time course as observed with the BOLD signal. Such comparisons will be of great importance to establish a link between haemodynamic changes measured by fMRI and underlying neural activity.

Acknowledgements

This work was supported by a grant “Imagerie du Petit Animal” from CNRS-CEA. We thank Jennifer Beshel for comments on the manuscript.

References

Abraham, N. M., Spors, H., Carleton, A., Margrie, T.W., Kuner, T., Schaefer, A.T., 2004. Maintaining accuracy at the expense of speed: stimulus similarity defines odor discrimination time in mice. Neuron 44, 865-876.

Buonviso, N., Amat, C., Litaudon, P., Roux, S., Royet, J.P., Farget, V., Sicard, G., 2003. Rhythm sequence through the olfactory bulb layers during the time window of a respiratory cycle. Eur. J. Neurosci. 17, 1811-1819.

Buonviso, N., Amat, C., Litaudon, P., 2006. Respiratory modulation of olfactory neurons in the rodent brain. Chem. Senses 31, 145-154.

Keilholz, S.D., Silva, A.C., Raman, M., Merkle, H., Koretsky, A.P., 2004. Functional MRI of the rodent somatosensory pathway using multislice echo planar imaging. Magn. Reson. Med. 52, 89-99.

Kida, I., Xu, F., Shulman, R.G., Hyder, F., 2002. Mapping at glomerular resolution: fMRI of rat olfactory bulb. Magn. Reson. Med. 48, 570-576.

Litaudon, P., Amat, C., Bertrand, B., Vigouroux, M., Buonviso, N., 2003. Piriform cortex functional heterogeneity revealed by cellular responses to odours. Eur. J. Neurosci. 17, 2457-2461.

Logothetis, N.K., Wandell, B.A., 2004. Interpreting the BOLD signal. Annu. Rev. Physiol. 66, 735-769.

Martin, C., Gervais, R., Hugues, E., Messaoudi, B., Ravel, N., 2004. Learning modulation of odor-induced oscillatory responses in the rat olfactory bulb: a correlate of odor recognition? J. Neurosci. 24, 389-397.

Rinberg, D., Koulakov, A., Gelperin, A., 2006. Speed-accuracy tradeoff in olfaction. Neuron 51, 351-358.

Royet, J-P., Jourdan, F., Ploye, H., Souchier, C., 1989. Morphometric modifications associated with early sensory experience in the rat olfactory bulb. II. Stereological study of the population of olfactory glomeruli. J. Comp. Neurol.. 289, 594-609.

Schafer, J.R., Kida, I., Rothman, D.L., Hyder, F., Xu, F., 2005. Adaptation in the rodent olfactory bulb measured by fMRI. Magn. Reson. Med. 54, 443-448.

Schafer, J.R., Kida, I., Xu, F., Rothman, D.L., Hyder, F., 2006. Reproducibility of odor maps by fMRI in rodents. Neuroimage 31, 1238-1246.

Spors, H., Grinvald, A., 2002. Spatio-temporal dynamics of odor representations in the mammalian olfactory bulb. Neuron 34, 301-315.

Spors, H., Wachowiak, M., Cohen, L.B., Friedrich, R.W., 2006. Temporal dynamics and latency patterns of receptor neuron input to the olfactory bulb. J. Neurosci. 26, 1247-1259.

Thévenet, M., Cheylus, A., 2003. Le logiciel ACTIVIS. Traitement et analyse d'images médicales 3D. Santé et Systémique 7, 191-199.

Uchida, N., Mainen, Z.F., 2003. Speed and accuracy of olfactory discrimination in the rat. Nat. Neurosci. 11, 1224-1229.

Wilson, D.A., 2000. Comparison of odor receptive field plasticity in the rat olfactory bulb and anterior piriform cortex. J. Neurophysiol. 84, 3036-3042.

Xu, F., Kida, I., Hyder, F., Shulman, R.G., 2000. Assessment and discrimination of odor stimuli in rat olfactory bulb by dynamic functional MRI. Proc. Nat. Acad. Sci. USA 19,

10601-10606.

Xu, F., Liu, N., Kida, I., Rothman, D.L., Hyder, F., Shepherd, G.M., 2003. Odor maps of aldehydes and esters revealed by functional MRI in the glomerular layer of the mouse olfactory bulb. Proc. Natl. Acad. Sci. USA 100, 11029-11034.

Yang, X., Hyder, F., Shulman, R.G., 1996. Activation of single whisker barrel in rat brain localized by functional magnetic resonance imaging. Proc. Natl. Acad. Sci. USA 93, 475-478.

Yang, X., Renken, R., Hyder, F., Siddeek, M., Greer, C.A., Shepherd, G.M., Shulman, R.G., 1998. Dynamic mapping at the laminar level of odor-elicited responses in rat olfactory bulb by functional MRI. Proc. Nat. Acad. Sci. USA 95, 7715-7720.

Figure legends

Figure 1: Stimulation protocol and analysis paradigm

Each fMRI run consisted of 60 volumes of 10 slices (1 sec per volume). Odour stimulation (isoamyl-acetate, 5 sec) was delivered after the acquisition of the 16^{th} volume of each run. The human canonical HRF (black curve) was used to set the epochs for our block design paradigm. Therefore, analysis consisted of contrast t-tests between the baseline period (volumes 1-16) and the stimulation period (volumes: 19-28)

Figure 2: Activation of the olfactory bulb in response to short odour stimulation

A: pattern of activation across the OB in response to 5 sec isoamyl-acetate stimulation from anterior (left) to posterior section (right). All the images were thresholded at the same value ($p<0.001$) Colour scale from $p=0.001$ (red) to $p<0.0001$ (yellow). Spatial scale: horizontal yellow bar=1 mm. B: Scan-to-scan BOLD response computed from one rat in dorso-lateral area (black lines) superimposed with mean BOLD response (red line). All the curves were normalized relative to the prestimulus period (volumes 1-16). C: Amplitude of BOLD responses along successive repetitions. Amplitudes were normalized relative to the first stimulus presentation. D: Areas of activation revealed by contrast t-statistic between baseline and stimulation period (left) and areas of activation revealed by correlation analysis with human canonical HRF (right). Both images were thresholded at $p=0.001$. E: Superimposition of canonical HRF (red line) and mean BOLD response (black line) computed by averaging the signals of all voxels within the dorso-lateral activation area (see Fig. 2A).

Figure 3: Temporal dynamics of OB activation

A: Normalized mean BOLD responses computed from all rats (n=6) in the three areas of activation. Black box: odour stimulation. B: Distribution of mean latency (±SD) in the three ROI. Numbers (from 1 to 6) show single data points for each animal.

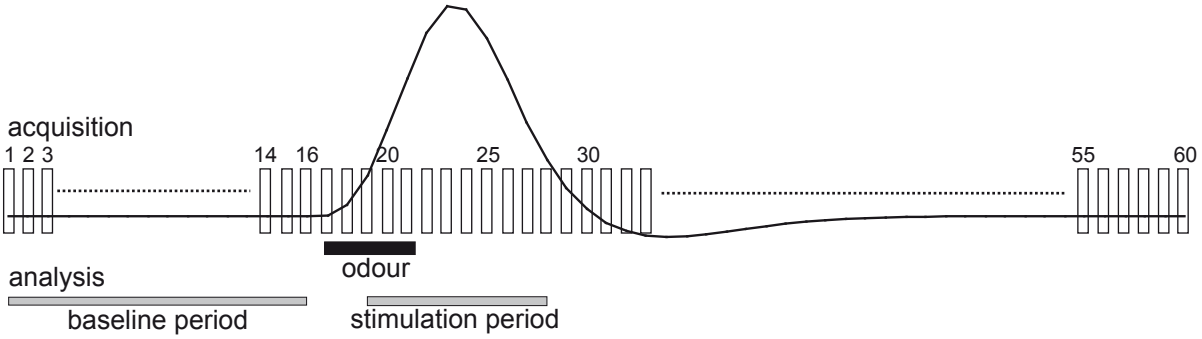
acquisition
1 2 3
14
16
20
25
30
55
60
odour
analysis
baseline period
stimulation period

Figure 1

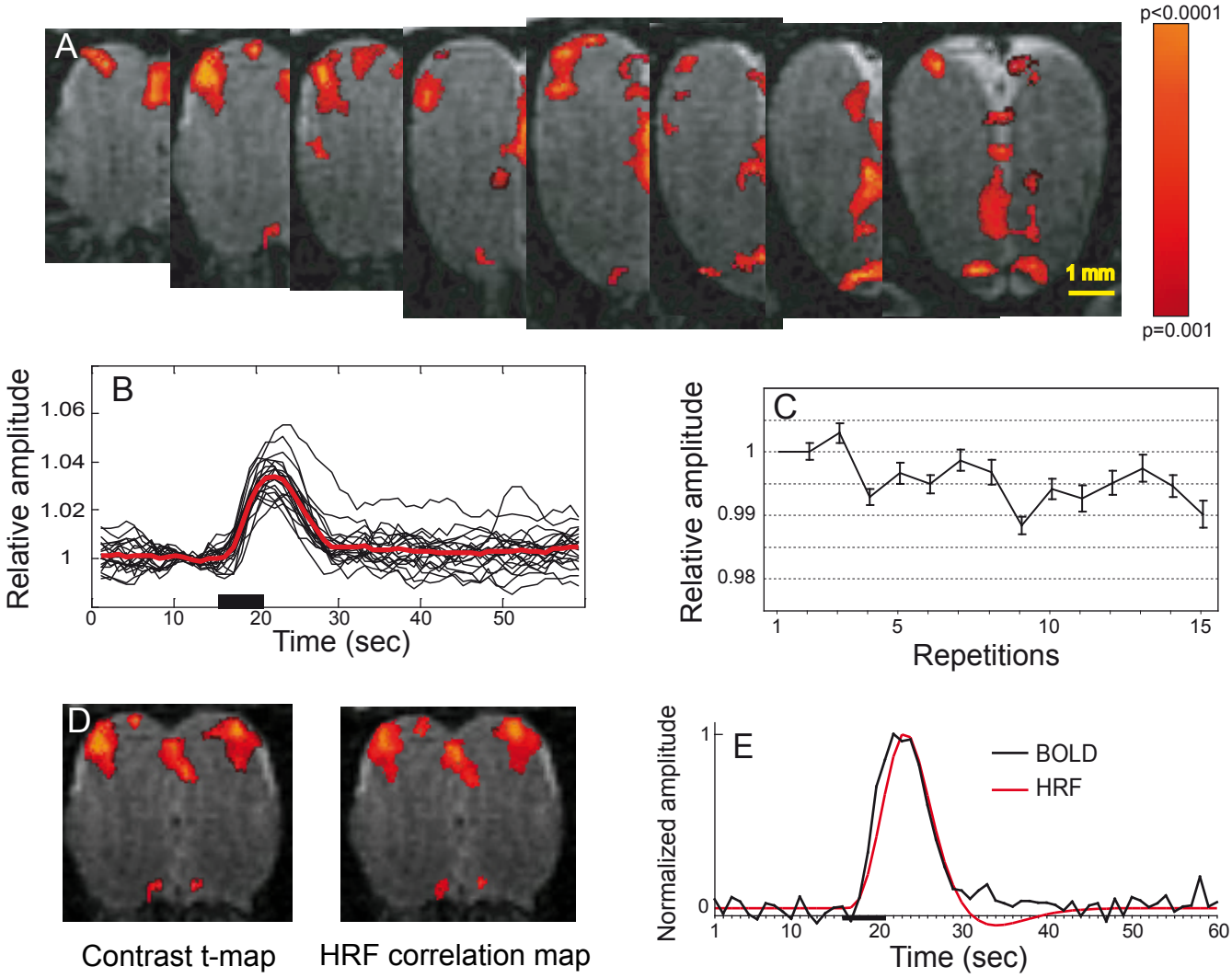
A
p<0.0001
p=0.001
1 mm
B
Relative amplitude
1.06
1.04
1.02
1
0
10
20
30
40
50
Time (sec)
C
Relative amplitude
1
0.99
0.98
1
5
10
15
Repetitions
D
Contrast t-map
HRF correlation map
E
Normalized amplitude
1
0
BOLD
HRF
1
10
20
30
40
50
60
Time (sec)

Figure 2

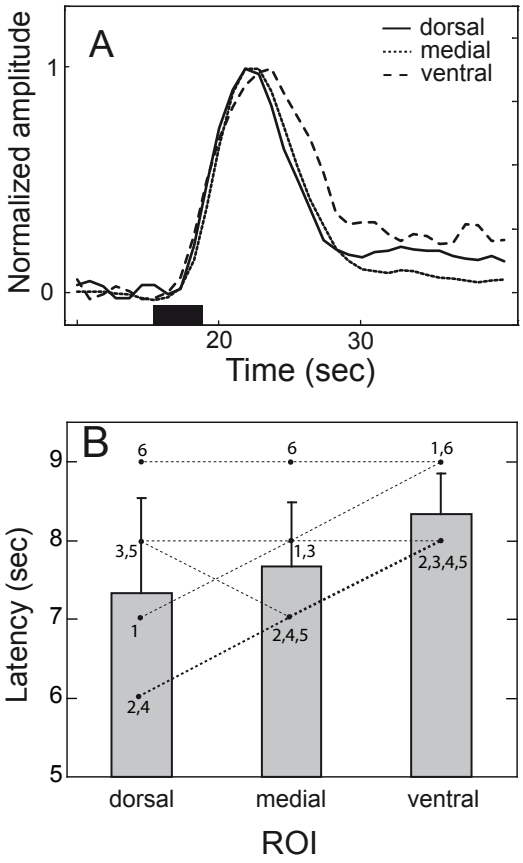
A
dorsal
medial
ventral
Normalized amplitude
1
0
20
30
Time (sec)
B
6
6
1,6
3,5
1,3
2,3,4,5
1
2,4,5
2,4
9
8
7
6
5
Latency (sec)
dorsal
medial
ventral
ROI

Figure 3